Numerical study on drag and lift coefficients of a marine riser at high Reynolds number using COMSOL multiphysics

M Faizal Ahmad[1a], Mohd Ridza Mohd Haniffah[2], Ahmad Kueh[3], Erwan Hafizi Kasiman[4]

[1] School of Civil Engineering, Faculty of Engineering, Universiti Teknologi Malaysia, 81310 UTM Johor Bahru, Malaysia
[2] UTM Centre for Industrial and Applied Mathematics (UTM-CIAM), Universiti Teknologi Malaysia, 81310 UTM Johor Bahru, Malaysia
[3] Department of Civil Engineering, Faculty of Engineering, Universiti Malaysia Sarawak (UNIMAS), 94300 Kota Samarahan, Sarawak, Malaysia

Email: [a] faizal_9273@yahoo.com

Abstract. Flow around a marine riser in water at the drag crisis regime was investigated using numerical modelling. In this regime, the drag coefficient drops off at a certain Reynolds number due to a change from laminar to turbulent flow. The aim is to investigate the capability of turbulence model to predict drag coefficient through COMSOL Multiphysics, a computational fluid dynamic (CFD) transient solver and compared against existing numerical models and experiment by Maritime Research Institute Netherlands (MARIN). Numerically, drag and lift forces depend on the point of separation from the cylinder in which different turbulence modelling will result in varying separation point and will lead to different vortex formation and the drag force. Reynolds Average Navier-Stokes (RANS) was employed using the k-ε and Menter's Shear Stress Transport (SST) turbulence model in two-dimensional CFD simulation. Six Reynolds numbers, similar to the test case, were considered. It can be concluded that the standard k-ε turbulence model, can only provide a good approximation at high turbulence regime, which is Reynolds number of 3.15×10^5 and higher. While, SST turbulence model can provide a good approximation at subcritical regime which before the sudden drop of drag force regimes.

1. Introduction

Flow field over a smooth circular cylinder in water has been a major benchmarking study in the past 50 years due to its relevance to many engineering applications. There are many examples of applications, for instance the circular piers in a river, marine piling, marine riser, pipeline, and cable on seabed. Although the circular shape geometry is simple, to model the vortex dynamics using computational fluid dynamics (CFD) methods are quite challenging. They are due to the flow instabilities in the wake region, in the boundary layer and the separating shear layer. The transition from laminar flow to turbulent flow and the boundary layer separation points depend on the Reynolds number. Detailed explanation on vortex dynamics in the cylinder wake can be found in the work of Williamson [1].

The drag crisis phenomenon occurs around critical Reynolds numbers $2 \times 10^5 - 5 \times 10^5$, where the averaged drag coefficient drops drastically since the boundary layer changes from laminar flow to turbulent flow and the flow separates further downstream. Studies have been carried out to investigate on the drag crisis phenomenon using experimental and numerical methods. For example, Farell and Blessmann [2] and Bearman [3] conducted experiments on flow around a circular cylinder at a range

of the critical Reynolds numbers. Similar tests were also conducted at a large range of Reynolds numbers, $6 \times 10^4 – 5 \times 10^6$, by Achenbach [4]. In addition, De Wilde and Huijsmans [5] carried out high Reynolds number vortex-induced vibration experiment using towing tanks with a fixed smooth circular cylinder. All the experimental results show that a significant drag loss occurred at Reynolds number $10^4 – 10^6$.

Apart from experimental modelling, numerical simulation is also applied actively on flow around cylindrical objects; specifically to understand drag crisis phenomenon of stationary or forced cylinders. An extensive research on the critical regime was done by Qiu et al. [6]. They were numerically studied drag and lift coefficients of a marine riser at high Reynolds numbers to benchmark the capabilities of computational fluid dynamic (CFD) methods through quantitative comparisons and validation studies against the test results of a circular cylinder. Seven CFD solvers, which are FLUENT, SNUFOAM, CFDShip-IOWA, Code-S, OpenFoam, Naoe-FOAM-SJTU, and STAR-CCM+ were used employing the Reynolds Averaged Navier Stokes (RANS), Detached Eddy Simulation (DES), and Large Eddy Simulation (LES). The simulations were varied according to Reynolds numbers ranging from $6.31 \times 10^4 – 7.57 \times 10^5$. Numerical predictions by LES are generally better than Unsteady RANS and DES at most Reynolds numbers. Meanwhile, Vaz et al. [7] carried out both two-dimensional and three-dimensional simulations for a stationary smooth circular cylinder using ANSYS-CFX10 with various turbulence models. The drag loss in the critical region was however not well captured.

The aim of this study is to investigate the capability of COMSOL Multipyhsics, a computational fluid dynamic (CFD) transient solver through quantitative comparisons against existing numerical models and experiment by Maritime Research Institute Netherlands (MARIN). The Menter's Shear Stress Transport (SST) and *k-ε* turbulence model were employed in two-dimensional RANS simulation. RANS is a more practical option as compared to DES and LES because of the computational cost and reliable result. Six Reynolds numbers, similar to the test case, were considered. The predicted averaged drag coefficients and the RMS values of lift coefficients are presented and compared with existing data.

2. Numerical methods

In the simulation of the unsteady viscous flow around a fixed smooth circular cylinder, the fluid is Newtonian and incompressible. Two-dimensional RANS model was employed in this work to give closure to the additional turbulent parameter, the Reynolds stress. The theoretical aspects of the computational methods are summarized below.

2.1 Governing equation

The governing RANS equations for the two-dimensional incompressible viscous flow consist of the continuity equation and the momentum equations as follows:

Continuity

$$\frac{\partial u_i}{\partial x_i} = 0 \tag{1}$$

Momentum

$$\rho \frac{\partial u_i}{\partial t} + \rho u_j \frac{\partial u_i}{\partial x_j} = -\frac{\partial p}{\partial x_i} + \frac{\partial}{\partial x_j}\left[\mu\left(\frac{\partial u_i}{\partial x_j} + \frac{\partial u_j}{\partial x_i}\right)\right] + \frac{\partial}{\partial x_j}\left(-\rho u_i' u_j'\right) \tag{2}$$

where $\rho u_i' u_j'$ is the Reynolds stress, which is then solved using eddy-viscosity model based on the Boussinesq assumption or solved from the transport equations based on Reynolds stress models.

$$-\rho u_i' u_j' = \mu_t\left(\frac{\partial u_i}{\partial x_j} + \frac{\partial u_j}{\partial x_i}\right) - \frac{2}{3}\rho k \delta_{ij} \tag{3}$$

where μ_t the turbulent or eddy viscosity and k is the turbulent kinetic energy.

The turbulent kinetic energy, k, can be solved from the transport equation, and the turbulence dissipation rate, ε, or the specific dissipation rate, ε/k, can be solved from the transport equations in turbulence models such as k-ε and k-ω models.

3. Numerical set-ups

A fixed circular cylinder with diameter of d = 0.1 m was constructed in COMSOL Multiphysics, which solves the Navier-Stokes equations via the finite element method. Following the set-up of MARIN as explain by Qiu et al. [6], the designed domain was shortened to 1.1 m high and 3.5 m long in order to reduce the simulation time. The center of the circular cylinder was located horizontally at the middle at 0.55 m from the water inlet of the domain as in figure 1. The density and the dynamic viscosity of the fluid are 1000 kg/m^3 and 1 × 10^{-3} kg/ms, respectively.

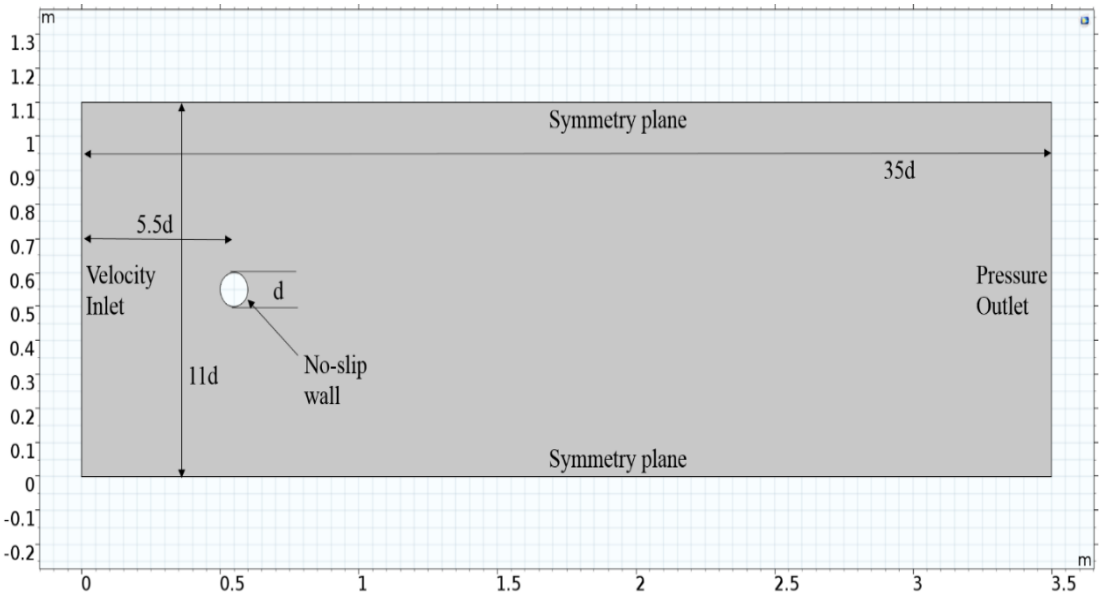

Figure 1. Computational domain dimension with boundary condition.

The velocity boundary condition, an uniform normal inflow with the velocity was specified on the inlet. The pressure boundary condition was applied on the outlet boundary which is sufficiently far from the cylinder for allowing the wake to dissipate naturally. Symmetric boundary conditions were set on two side boundaries to avoid flow disturbance from the side boundaries. No-slip wall boundary condition was specified on the lines of circle.

Triangular unstructured grids were generated with refinement close to the circumference of the circle. Note that very fine rectangular structured grids were used around the circle in order to capture the boundary layers. The global view and a close-up of the rectangular structured grids around the circle are presented in figure 2a and figure 2b.

Simulations were carried out for six in-flow velocities, corresponding to the Reynolds numbers ($Re = \rho Ud/\mu$). The normal inflow velocity was varied as 0.631, 1.26, 2.52, 3.15, 5.06 and 7.57 m/s, corresponding to Reynolds number of 0.631, 1.26, 2.52, 3.15, 5.06 and 7.57 x 105, respectively. Note that these Reynolds numbers are in the sub-critical, the critical and the super-critical regimes. The hydrodynamic drag and lift coefficients were calculated by using the Morison equation [8],

$$C_D = \frac{F_D}{0.5\rho U^2 A} \tag{4}$$

where ρ is the fluid density, A is the projected frontal area or line, U is the free-stream velocity, and F_D is the drag force computed by the numerical simulation.

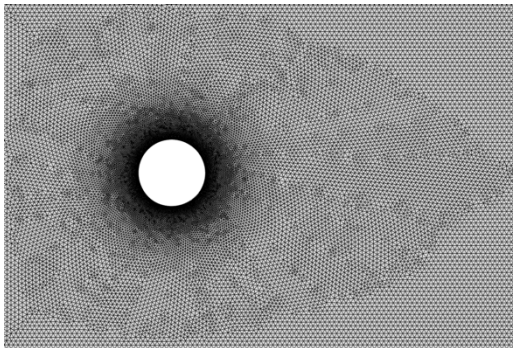

Figure 2a. Global view.

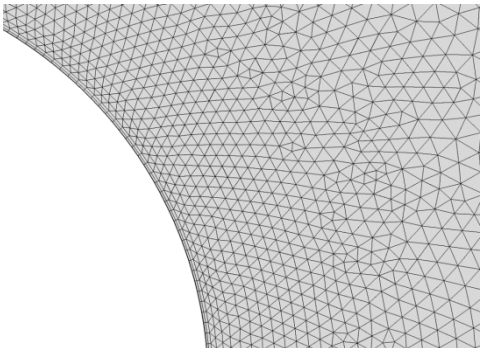

Figure 2b. Close-up view.

Seven CFD solvers were used by previous researchers to simulate the flow field around a smooth cylinder with the same Reynolds number. The comparison of the numerical methods including the current study details associated with the computational details are presented in Table 1a and Table 1b.

4. Result and discussion

Figure 3 shows the variation of mean C_D as a function of Reynolds numbers for all considered numerical and experimental results. The mean C_D of the *k-ε* model simulation using COMSOL Multiphysics was found gradually decrease from 0.45 to 0.31 at Reynolds numbers of 1.26 x 10^5 to 7.57 x 10^5. The experimentally obtained C_D of MARIN dropped from 1.16 to 0.26 as the Reynolds numbers increase, which means a change in regime from subcritical to critical where the mean C_D started to drop into supercritical regime. The mean C_D of the SST model produced same graph pattern to experimental results. As can see, SST model also shows the sudden drop at the same Reynolds numbers of experimental which is in between Reynolds number of 2.52 x 10^5 to 3.15 x 10^5. However, the model was overestimated mean C_D at critical and supercritical regimes.

The relative errors of the *k-ε* model for the mean C_D are 65, 60, 49, 39, 31 and 19% for the Reynolds numbers of 0.631, 1.26, 2.52, 3.15, 5.06, and 7.57 × 10^5, respectively, compared to experimental results. Meanwhile, the relative errors of the SST model for the mean C_D are 32, 25, 37, 200, 225 and 150% for the same Reynolds numbers. Therefore, it shows that the *k-ε* model outcomes are low accuracy compared to other simulation for both subcritical and critical regimes. While, it performed well for the supercritical regime, ranked as the second-best simulation platform after CFDShip-IOWA compared to others as in Figure 3. In contrast, SST model performed poorly in supercritical regime, which the relative errors up to 150% and above.

Table 1a. Numerical methods and computational details of previous studies [6] and current study.

	Code name	**2D/3D**	**RANS/DES/LES**	**Number of Grid**	**Type of Grid**	**Convection Term**
A	FLUENT (Commercial Code)	2D	RANS	87,223	Structured	Upwind
B	SNUFOAM (In-house Code)	2D	RANS	32,280	Structured	Upwind
C	FLUENT (Commercial Code)	2D	RANS	43,820	Structured	Upwind
D	CFDShip-IOWA (In-house Code)	3D	LES	67,000,000	Structured	QUICK/ WENO
E	Code-S (In-house Code)	3D	LES	11,300,000	Unstructured (Cartesian)	Upwind
F	OpenFOAM (Open Source Code)	3D	LES	Max 4,000,000	Unstructured	Hybrid (Central + Upwind)
G	Naoe-FOAM-SJTU (In-house Code)	2D	RANS	100,000	Chimera	Upwind
H1	STAR-CCM+ (Commercial Code)	2D	RANS	592,478	Hybrid	Upwind
H2	STAR-CCM+ (Commercial Code)	2D	RANS	592,478	Hybrid	Upwind
H3	STAR-CCM+ (Commercial Code)	3D	DES	12,400,000	Structured	Upwind
H4	STAR-CCM+ (Commercial Code)	3D	LES	12,400,000	Structured	Upwind
COMSOL1	COMSOL (Commercial Code)	2D	RANS	215,248	Unstructured	Upwind
COMSOL2	COMSOL (Commercial Code)	2D	RANS	215,248	Unstructured	Upwind

Table 1b. Numerical methods and computational details of previous studies [6] and current study.

	Code name	**Δt**	**y+**	**Wall Function (Used/Not Used)**	**Turbulence Model**	**Aspect Ratio (AR)**
A	FLUENT (Commercial Code)	0.001/0.005	59	U	*k-ω* SST	-
B	SNUFOAM (In-house Code)	0.001/0.002/ 0.0001	2	N	*k-ω* SST	-
C	FLUENT (Commercial Code)	0.001	10	N	*k-ω* SST	-
D	CFDShip-IOWA (In-house Code)	0.00008/0.0001	0.03~0.15	N	Dynamic model	2 and 8
E	Code-S (In-house Code)	(CFL=0.5)	-	N	Dynamic model	π
F	OpenFOAM (Open Source Code)	0.005	1	N	Dynamic model	1.7, π, 2π
G	Naoe-FOAM-SJTU (In-house Code)	0.00017 ~ 0.0015	1~4.9	U	*k-ω* SST	-
H1	STAR-CCM+ (Commercial Code)	0.0001 ~ 0.002	0.06~0.56	N	*k-ω* SST	-
H2	STAR-CCM+ (Commercial Code)	0.0001 ~ 0.002	0.06~0.56	N	*k-ε* (Standard)	-
H3	STAR-CCM+ (Commercial Code)	0.002 ~ 0.02	0.06~0.56	N	-	3
H4	STAR-CCM+ (Commercial Code)	0.002 ~ 0.02	0.06~0.56	N	-	12
COMSOL1	COMSOL (Commercial Code)	0.0009 ~ 0.0062	8.7~40	U	*k-ω* SST	-
COMSOL2	COMSOL (Commercial Code)	0.02	11~69	U	*k-ε* (Standard)	-

According to Cengel and Cimbala [9], mean C_D of 2D cylinder simulation is 1.2 for Reynolds numbers ranges from 1×10^4 to 2×10^5 which is laminar flow or subcritical regime and 0.3 for turbulent flow which mean supercritical regime. Consequently, the relative errors of SST simulation model were reduced to 28 and 15% for Reynolds numbers of 6.31×10^4 and 1.26×10^5 respectively, when compared to the mean C_D of 1.2. While, the relative errors of *k-ε* model were reduced to 25 and 14 for Reynolds numbers of 3.15 x 10^5 and 5.06 x 10^5 respectively compared to 0.3 mean C_D.

Figure 3 illustrates that both models simulated using standard *k-ε* turbulence model (H2 and COMSOL2) were fluctuated at a certain value of the mean C_D, which does not show any drop from the subcritical to supercritical regimes as displayed by both the theoretical and experimental plots. According to Zhang [10], the standard *k-ε* turbulence model is not suitable for drag force analysis because of the dissipation rate of the turbulence energy (epsilon) equation contains a specific term, which cannot be calculated at the wall of the blunt body. Therefore, wall functions must be used in the model in order to get better accuracy.

COMSOL Multiphysics SST model shows better performance at subcritical regimes which Reynolds number ranging from 6.31 x 10^4 – 2.52 x 10^5. SST model also shows sudden drop at the critical regime which is Reynolds number 3.15 x 10^5 as shown as experimental results, but the errors for critical and supercritical regimes are very large compared to experimental results. This is due to its assumption of the model in which SST model is one of low Reynolds turbulence model. Therefore, SST model is suitable for subcritical flow regime where the assumption of the model is similar and valid.

As can see, the blue dash line is combination results of the two turbulence model which is *k-ε* and SST model. Reynolds number ranging from 6.31 x 10^4 – 2.52 x 10^5 using SST model results and *k-ε* model results for Reynolds numbers ranging from 3.15 x 10^5 – 7.57 x 10^5. This combination made the simulation results satisfied experimental data which the sudden drop is more obvious and the relative errors were reduced. SST model is a low Reynolds turbulence model that perfect for laminar flow or subcritical regime, while *k-ε* model is a high Reynolds turbulence model that perfect for turbulent flow or supercritical regime. Transition flow or critical regime is where the flow condition that very difficult for RANS model to simulate because of its flow behavior is very complex.

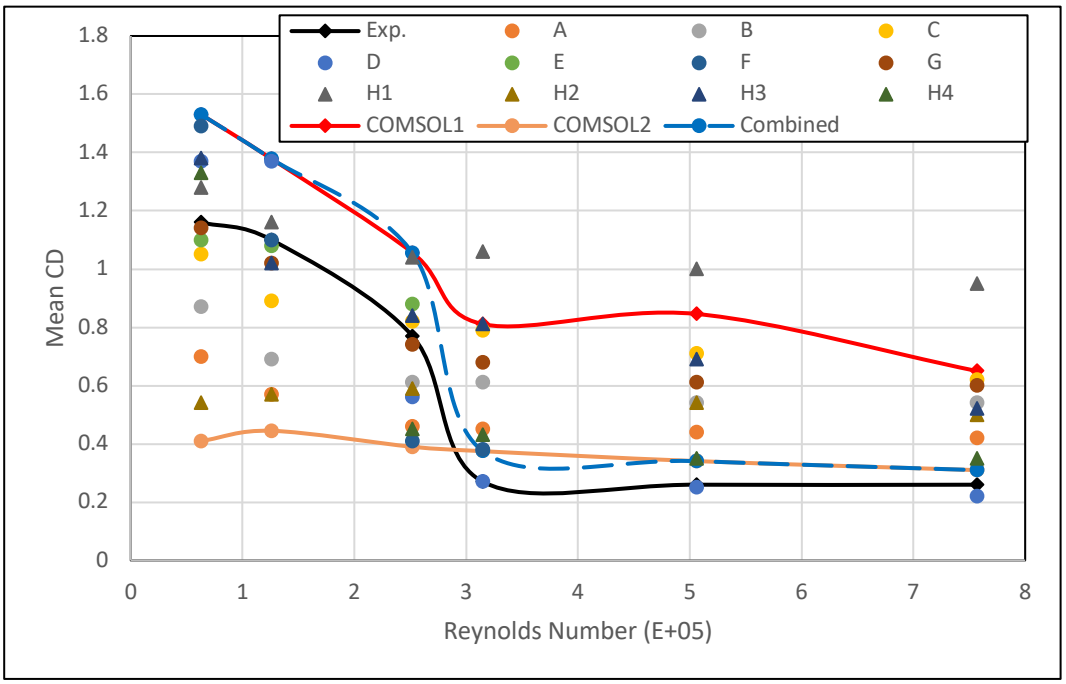

Figure 3. Mean drag coefficient from various numerical studies and experimental outcome (adapted from Qiu et al., [6]) vs current method

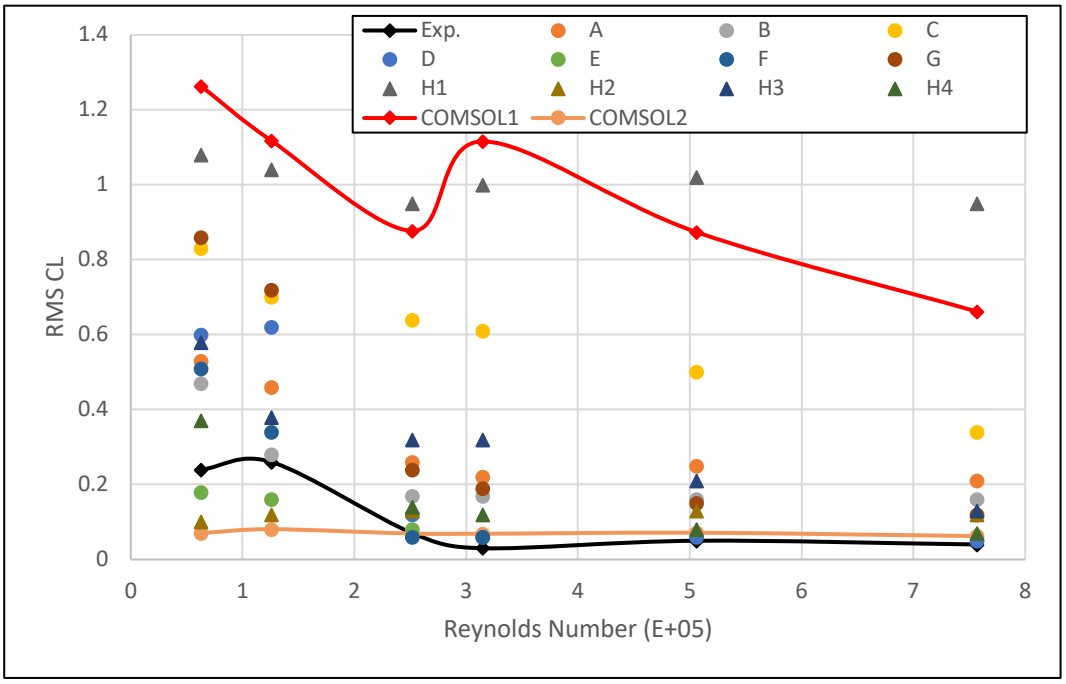

Figure 4. Root mean square lift coefficients from various numerical studies and experimental outcome (adapted from Qiu et al., [6]) vs current method

Figure 4 shows the variation of $RMSC_L$ as a function of Reynolds numbers from all numerical studies, experimental results from Qiu et al., [6] and current study. The $RMSC_L$ of the *k-ε* model was found to be constant around 0.06 to 0.08 for all Reynolds numbers. Since, the vortex shedding at the leeward of the cylinder are formed quite far away behind, the induced upward and downward forces are weaker.

The relative errors of the standard *k-ε* model for $RMSC_L$ were 71, 69, 1, 129, 43 and 56 for the Reynolds numbers of 0.631, 1.26, 2.52, 3.15, 5.06, and 7.57 × 10^5, respectively, compared to the experimental results by MARIN. Whereas, the relative errors of SST model for $RMSC_L$ were up to 330% and above for the same Reynolds numbers. *K-ε* model has performed well to simulate water flow around a cylinder in the supercritical regime or turbulent flow for both mean C_D and $RMSC_L$ as it is a high Reynold turbulence model.

COMSOL Multiphysics SST model has over predicted the value of $RMSC_L$ of the fluid flow around a cylinder compared with experimental results. The significant value of forces in vertical direction due to horizontal vortices are formed along the cylinder. In SST model, large vortices are formed and its alternating between clockwise and anticlockwise due to the symmetrical shape of circular cylinder. As the assumption of the SST model, strong recirculation and curvature are formed as its low Reynolds turbulence model even at supercritical regimes.

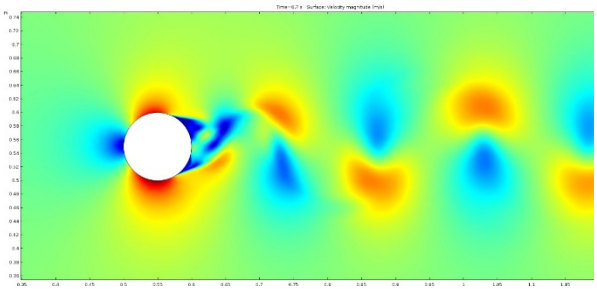

Figure 5a. Velocity field of SST model at Reynolds number 7.57 x 10^5.

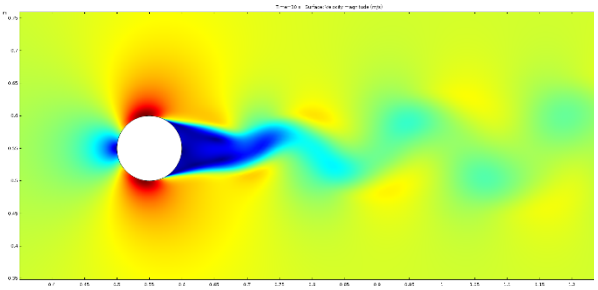

Figure 5b. Velocity field of *k-ε* model at Reynolds number 7.57 x 10^5.

As shown in Figure 5a and Figure 5b, different turbulence model will produce different flow field of water flow around a cylinder in 2D at same Reynolds number and mesh structure. Both models generate vortex shedding at leeward of the cylinder, but both have obviously different patent of wake. SST more effective in capture or simulate the curvature of the flow. Meanwhile, *k-ε* turbulence model cannot capture the curvature around the blunt-body or cylinder. As the high Reynolds turbulence model, *k-ε* model showed flow field of inviscid flow around a cylinder while SST model, a low Reynolds turbulence model produces more complex of wake pattern due to considering the viscosity of the fluids in the physics of model.

5. Conclusion

Turbulent flow around a stationary marine riser with a circular cylinder shape was simulated at various Reynolds numbers in the subcritical, critical, and supercritical regimes by using the standard *k-ε* and SST turbulence model in the COMSOL Multiphysics platform. The focus was to investigate the capability of both models by comparing the mean drag coefficient and root mean square (RMS) lift coefficient to the benchmark experimental data of a stationary circular cylinder as provided by the Maritime Research Institute of Netherlands (MARIN). It can be concluded that, the simulation using the standard *k-ε* turbulence model is capable to represent the true mean C_D and $RMSC_L$ of water flow around a cylinder at the supercritical regime for the Reynolds number of 3.15×10^5 and higher. Meanwhile, the simulation using SST turbulence model is capable to represent drag and lift forces of water flow around a cylinder as the subcritical regimes which before the sudden drop of drag force regimes.

Acknowledgement

This research was financially supported by the Malaysian Ministry of Education (MOE) under the Research University Grant (GUP) of Universiti Teknologi Malaysia Q.J130000.2522.17H27.

References

[1] Williamson C H 1996 *Annual review of fluid mechanics* **28**(1) 477-539
[2] Farell C and Blessmann J 1983 *Journal of Fluid Mechanics* **136** 375-391
[3] Bearman, P W 1969 *Journal of Fluid Mechanics* **37**(3) 577-585
[4] Achenbach E 1968 *Journal of Fluid Mechanics* ***34***(4) 625-639
[5] De Wilde J J and Huijsmans R H M 2001 Experiments for high Reynolds numbers VIV on risers. In *The Eleventh International Offshore and Polar Engineering Conference*. International Society of Offshore and Polar Engineers
[6] Qiu W, Lee D Y, Lie H, Rousset J M, Mikami T, Sphaier S, Tao L, Wang X and Magarovskii V, 2017 *Applied Ocean Research* **69** 245-251
[7] Vaz G, Mabilat C, van der Wal R, and Gallagher P 2007 Viscous flow computations on a smooth cylinders: a detailed numerical study with validation. In *ASME 2007 26th International Conference on Offshore Mechanics and Arctic Engineering* (pp. 849-860). American Society of Mechanical Engineers.
[8] Morison J R, Johnson J W, and Schaaf S A 1950 *Journal of Petroleum Technology* **2**(05) 149-154.
[9] Cengel Y and Cimbala J 2013 *Fluid Mechanics: Fundamentals and Applications.* The McGraw-Hill Companies, Inc.
[10] Zhang D 2017 *Journal of Physics: Conference Series* **910**.